scientific reports

OPEN

Development of actionable targets of multi-kinase inhibitors (AToMI) screening platform to dissect kinase targets of staurosporines in glioblastoma cells

Oxana V. Denisova[1], Joni Merisaari[1,2], Amanpreet Kaur[1], Laxman Yetukuri[1,3], Mikael Jumppanen[1], Carina von Schantz-Fant[3], Michael Ohlmeyer[4,5], Krister Wennerberg[3,6], Tero Aittokallio[3,7,8], Mikko Taipale[9] & Jukka Westermarck[1,2✉]

Therapeutic resistance to kinase inhibitors constitutes a major unresolved clinical challenge in cancer and especially in glioblastoma. Multi-kinase inhibitors may be used for simultaneous targeting of multiple target kinases and thereby potentially overcome kinase inhibitor resistance. However, in most cases the identification of the target kinases mediating therapeutic effects of multi-kinase inhibitors has been challenging. To tackle this important problem, we developed an actionable targets of multi-kinase inhibitors (AToMI) strategy and used it for characterization of glioblastoma target kinases of staurosporine derivatives displaying synergy with protein phosphatase 2A (PP2A) reactivation. AToMI consists of interchangeable modules combining drug-kinase interaction assay, siRNA high-throughput screening, bioinformatics analysis, and validation screening with more selective target kinase inhibitors. As a result, AToMI analysis revealed AKT and mitochondrial pyruvate dehydrogenase kinase PDK1 and PDK4 as kinase targets of staurosporine derivatives UCN-01, CEP-701, and K252a that synergized with PP2A activation across heterogeneous glioblastoma cells. Based on these proof-of-principle results, we propose that the application and further development of AToMI for clinically applicable multi-kinase inhibitors could provide significant benefits in overcoming the challenge of lack of knowledge of the target specificity of multi-kinase inhibitors.

Multi-kinase inhibitors (MKIs) and more targeted kinase inhibitors are often used in cancer therapies without exact knowledge of the kinases targeted for the therapeutic benefit[1–4]. Staurosporines (STSs) are a large family of MKIs originally derived from bacterial alkaloid staurosporine[5]. STSs function as classical ATP mimics and are known to inhibit up to 50 kinases with approximately similar efficacy[1,4,5]. Regardless of their very wide target spectrum and reputation as "dirty kinase inhibitors" several STS derivatives have reached or have been tested in the clinics. Midostaurin (PKC412) is approved for the treatment of FLT3-mutated acute myeloid leukemia[2], whereas another STS derivative UCN-01 (7-hydroxystaurosporine) was tested in phase II clinical trials in metastatic melanoma and relapsed T-Cell Lymphomas (NCT00082017). However, actual targets that mediate the therapeutic effect are not well established. Further, in a case of brain tumors STS derivatives are compromised by their pharmacokinetic properties as they do not cross the brain-blood barrier (BBB).

Development of MKIs towards clinical use would benefit from a better understanding of the kinase targets mediating both the therapeutic and potential toxic effects in each disease application. However, generalizable strategies for the analysis of actionable MKI targets are currently missing. Here, we present Actionable Targets of Multi-kinase Inhibitors (AToMI) as a generalizable approach to identifying actionable co-targets of MKIs.

[1]Turku Bioscience Centre, University of Turku and Åbo Akademi University, Turku, Finland. [2]Institute of Biomedicine, University of Turku, Turku, Finland. [3]Institute for Molecular Medicine Finland, HiLIFE, University of Helsinki, Helsinki, Finland. [4]Icahn School of Medicine at the Mount Sinai, New York, NY, USA. [5]Atux Iskay LLC, Plainsboro, NJ, USA. [6]Biotech Research and Innovation Centre, University of Copenhagen, Copenhagen, Denmark. [7]Centre for Biostatistics and Epidemiology, University of Oslo, Oslo, Norway. [8]Institute for Cancer Research, Oslo University Hospital, Oslo, Norway. [9]Donnelly Centre, University of Toronto, Toronto, Canada. ✉email: jukwes@utu.fi
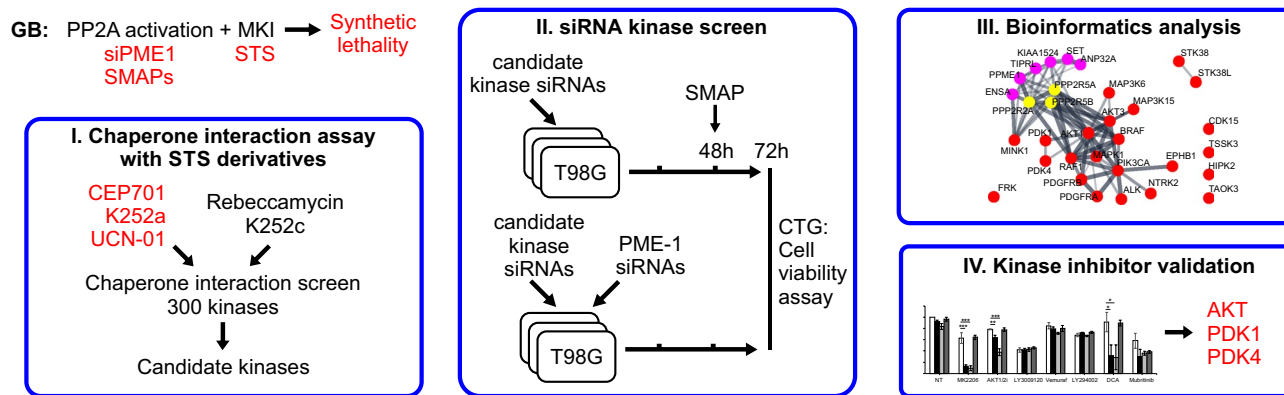
Figure 1. A schematic illustration of AToMI screening platform.

We propose that the application of AToMI for clinically applicable MKIs would provide significant benefits in overcoming the challenge of lack of knowledge of target specificity of kinase inhibitors.

Results

Strategy for the characterization of actionable targets of multi-kinase inhibitors (AToMI).
Protein phosphatase 2A (PP2A) inhibition drives resistance to several kinase inhibitors in multiple cancer types, therefore PP2A reactivation could be envisioned as a novel therapeutic opportunity to overcome kinase inhibitor resistance[6–9]. We hypothesized that combination of multi-kinase inhibition and PP2A reactivation would result in such a broad-spectrum inhibition of serine/threonine phosphorylation that cancer cells could not anymore use phosphorylation-dependent signaling rewiring as an escape mechanism. Related to glioblastoma (GB), we recently demonstrated strong synergistic activity between PP2A reactivation and clinically tested STS derivative UCN-01[10]. However, as UCN-01 targets approximately 50 different kinases at nanomolar concentrations[1,5] it remains unclear which one(s) of these kinases are involved in a synthetic lethality (SL) phenotype observed in combination with PP2A reactivation. To systematically map the UCN-01 co-target interactions relevant to synergy with PP2A reactivation, we devised a functional screening platform consisting of the following steps (Fig. 1):

(1) Chaperone interaction assay to compare direct kinase binding between UCN-01 and STS derivatives displaying differential synergism with PP2A reactivation in GB cells.
(2) siRNA screening for synergistic interaction between PP2A reactivation and targeting of the individual kinase hits from the step 1.
(3) Bioinformatics analysis of actionable kinase networks based on steps 1 and 2.
(4) Small molecule kinase inhibitor validation experiments.

As this strategy could be generally suitable for functional filtering of targets of MKIs, we hereby refer to the screening platform as characterization of Actionable Targets of Multi-kinase Inhibitors (AToMI). The individual technologies used in AToMI are interchangeable with the most suitable technologies for any other application AToMI would be used for.

Use of AToMI to identify actionable kinase targets of STSs synergizing with PP2A reactivation.
Using AToMI, we compared the kinase target profiles of STS derivatives UCN-01, CEP-701 and K252a, previously shown to synergize with PP2A reactivation, against STS derivatives K252c and rebeccamycin that did not synergize with PP2A reactivation[10]. The differential synergistic activities of these STS derivatives in combination with a small molecule activator of PP2A (SMAPs), NZ-8-061[11], were confirmed by colony growth assay in T98G cells (Fig. 2A). In the first step of AToMI, all five STS compounds were screened for their direct kinase protein binding against 355 kinases and their 176 mutants by a Chaperone interaction assay (Fig. 2B)[12]. This assay measures the interaction of kinases with their chaperone Cdc37 in the presence (or absence) of kinase inhibitors. Binding of the inhibitor to its target leads to thermodynamic stabilization of the target, which can be detected as a weaker interaction between the kinase and Cdc37[13]. Importantly, the assay can detect subtle changes in inhibitor binding caused by mutations found in patients, reflecting the cellular potency[13]. Using log2 50% reduction in chaperone binding as a threshold for interaction, a total of 29 candidate kinases were identified to differentially interact with STS derivatives that synergized with PP2A (CEP-701, K252a, and UCN-01), but not with rebeccamycin or K252c (Figs. 2C, S1, Tables S1, S2). Notably, 26/29 of the candidate kinases were previously known to be STS target kinases based on Drug Target Commons database (https://drugtargetcommons.fimm.fi/bioactivities?id=DTCC00444871&category=Compound&name=STAUROSPORINE).

In the siRNA screening step of AToMI, the goal was to identify among the shared targets of CEP-701, K252a, and UCN-01, individual kinases whose co-inhibition resulted in synergism with PP2A reactivation in cell viability inhibition. The screening was conducted using a custom human kinase siRNA library, which had three non-overlapping siRNAs targeting each kinase. In addition to the 29 candidate kinases from the step 1, the siRNA
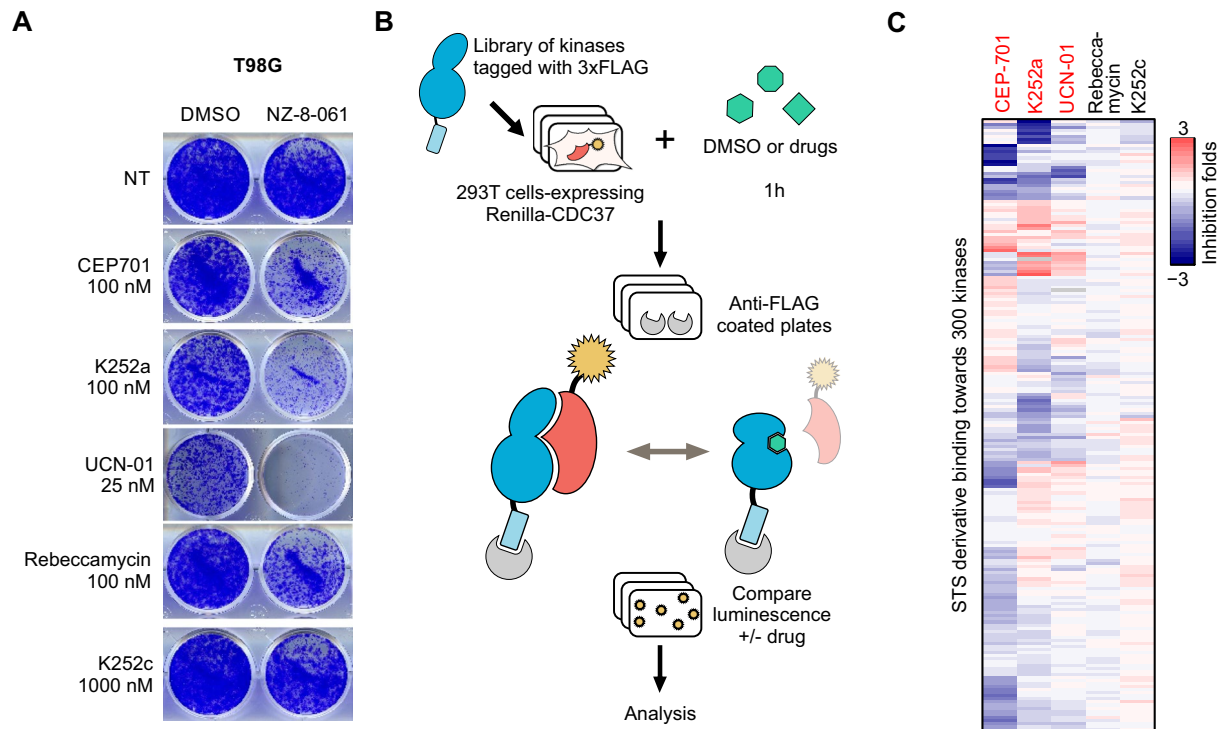
Figure 2. STS derivatives screening in Chaperone interaction assay. (**A**) Representative images of colony formation assay in T98G cells treated vehicle (DMSO) and NZ-8-061 in combination with STS derivatives. (**B**) A scheme of Chaperone interaction assay. Kinases tagged with 3xFLAG (blue), Renilla-CDC37 (red), tested drugs (green), anti-FLAG antibodies (grey). (**C**) Heat map representation of interaction of STS derivatives, CEP-701, K252a, UCN-01, rebeccamycin and K252c, with protein kinases by Chaperone interaction assay. STS derivatives causing synthetic lethality (red), no effect (black). Color scale bar indicates log2 fold changes of kinase/Cdc37 interactions between inhibitor and DMSO treatments.

library was extended with eight additional kinases either known to be STS targets but not represented in the used Chaperone interaction assay library or being frequently altered in GB[14–18] (Table S3). Importantly, although PKC could be considered as bona-fide STS target it was not included in the extended siRNA list, since no synergy was detected with PKC inhibitors Gö6976 and chelerythrine chloride and PP2A reactivation previously[10]. The siRNAs were reverse transfected into T98G cells, and the cells were subsequently exposed to PP2A reactivation by NZ-8-061 treatment (Fig. 3A). In the validation screen, we selected 25 kinases in combination with PME-1 siRNAs to evaluate the similarity in drug sensitization between chemical (NZ-8-061) and genetic (PME-1 siRNA) PP2A reactivations (Fig. 3A). The efficacy of PME-1 depletion by tree independent siRNAs was validated by western blotting from parallel samples (Fig. S2). For each kinase siRNA, Gene Activity Ranking Profiles and synergy scores were computed as described in the methods section of the siRNA screens. Notably, regardless of the marked differences in the targeting approaches, most of the kinases targeted in both screens were found to synergize with both NZ-8-061 treatment and PME-1 depletion (Fig. 3B), validating both the shared PP2A-induced mode of action, and the broad impact of PP2A activity in kinase inhibitor tolerance in GB.

STRING protein–protein interaction network analysis of the AToMI candidate kinases from the step 2 revealed enrichment of RTK/RAF/MAPK (PDGFR, RAF1, BRAF, and MAPK1) and PI3K/AKT/mTOR pathways (PIKCA, AKT1 and AKT3), as well as mitochondrial pyruvate dehydrogenase kinase (PDK1 and PDK4) among the kinases connected to PP2A B-subunits responsible for SL by STS treatment and PME-1 depletion (Fig. 3C)[10]. As each of these kinase modules were also represented among the kinases that were shared between the NZ-8-061 and siPME-1 synergy targets, we proceeded to test these GB signaling nodes using selective small-molecule inhibitors. Selectivity of the chosen small-molecule inhibitors was evaluated based on recently published target selectivity databases, and for some compounds also by the Chaperone interaction assay (Table S4)[1,4,19–21]. Additionally, allosteric inhibitors were prioritized. To facilitate potential future translation of the results, we considered the oral bioavailability and BBB permeability of the compounds in the drug selection based on published literature[22–24]. The selected seven kinase inhibitors were screened for cell viability effects in T98G cells with two SMAPs, NZ-8-061 and DBK-1154[25]. As a control, we used an inactive SMAP analog DBK-766, that binds PP2A but is unable to reactivate it even at a concentration of 20 μM in vitro[11]. The results show that both NZ-8-061 and DBK-1154 sensitized T98G cells to MK-2206 and AKT1/2i (AKT signaling)[26], and DCA (PDK inhibitor)[22,27] used at concentrations that engage their aimed target kinase (Fig. 4A, S3A, B). Importantly, the inactive SMAP (DBK-766) did not synergize with any of these kinase inhibitors (Fig. 4A) and another PDK inhibitor, lipoic acid[27], recapitulated the synergy with SMAPs (Fig. S3C, D). Further validating PP2A reactivation as the mechanism inducing the synergistic drug interaction, also PME-1 inhibition synergized with both
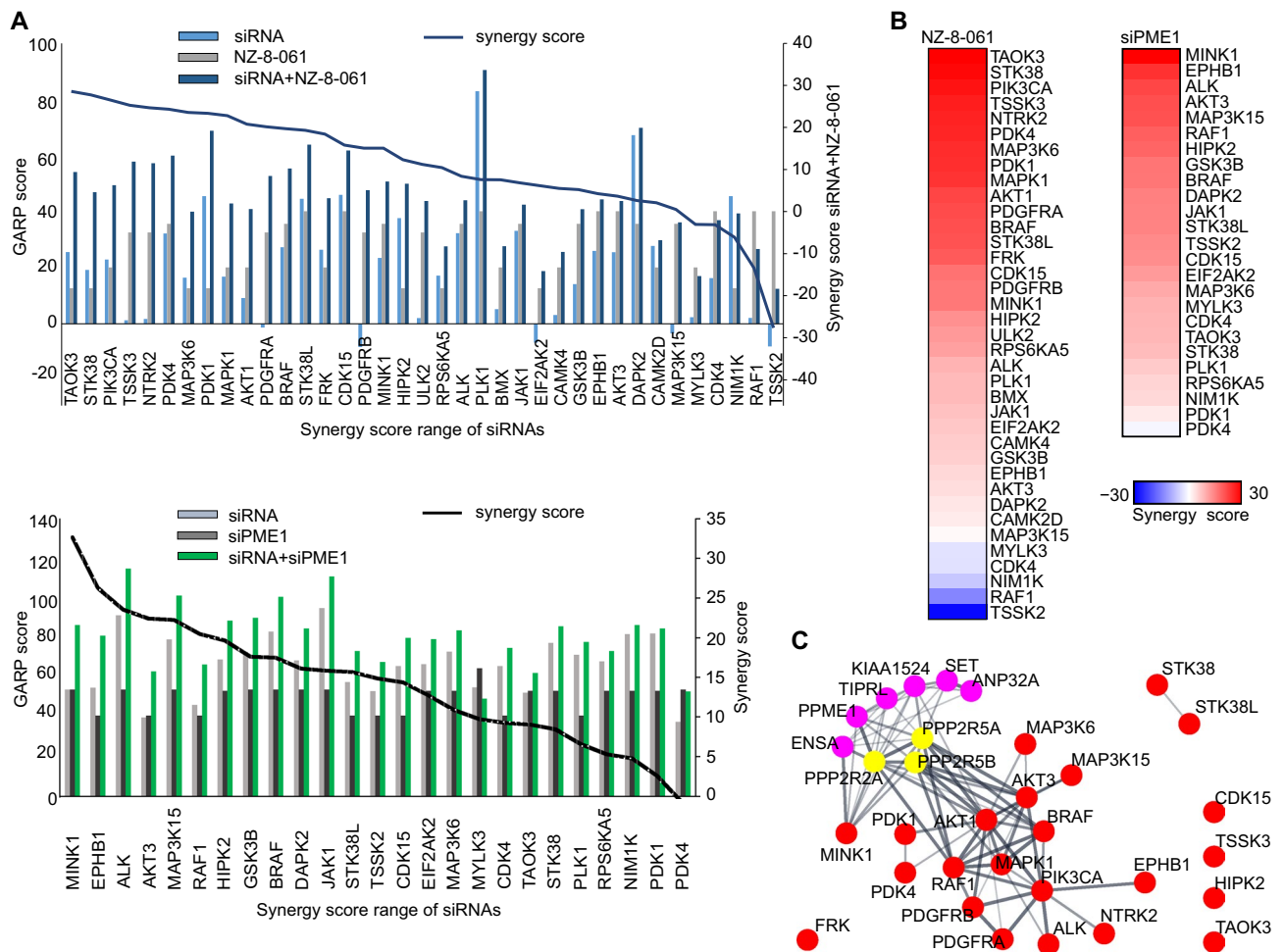
Figure 3. siRNA screening to kinases involved in GB cell synthetic lethality in combination with PP2A reactivation. (**A**) GARP scores of siRNA screen in T98G cells under NZ-8-061-treatment or PME-1 depletion (left axis). Kinases were ordered according to synergy scores of a siRNA (right axis). (**B**) Heat map representation of kinases involved in synthetic lethality in NZ-8-061-treated and PME-1-depleted T98G cells. Color bar indicates the synergy scores. (**C**) STRING interactive mapping of screen kinase hits onto PP2A network.

MK-2206 and DCA treatments (Fig. S3E). On the other hand, RAF inhibitors (LY3009120 and vemurafenib), PI3K inhibitor (LY294002), or MINK1 inhibitor (mubritinib) did not display significant combinatorial effects with PP2A reactivation (Fig. 4A).

Collectively, these results demonstrated the usefulness of AToMI screening for the identification of individual actionable target kinases for MKIs.

Exploration of AToMI results in heterogeneous GB cell lines. Cellular heterogeneity and high intrinsic therapy resistance of GB, as well as the presence of glioblastoma stem-like cells (GSCs) are major challenges related to GB therapies[28]. To explore relevance of AToMI results across GB cell lines, we applied AKT and PDK inhibitors in combination with SMAPs to two additional established GB cell lines, E98 and U87MG, and two patient-derived GSC lines, BT-CD133+ and BT12[25,29]. Consistently with the high intrinsic kinase inhibitor resistance of GB cells[25,30], none of the kinase inhibitor monotherapies used at doses that effectively inhibited their intended targets (Fig. S3A, B), induced a cytotoxic response (i.e. more than 50% reduction in cell viability) (Fig. 4B). Furthermore, illustrative of the challenge with heterogeneity of GB cell therapy responses, maximal inhibition of cell viability with any doublet combinations was highly variable across the cell lines. In example, BT-CD133+ cells were fully resistant to combination of AKT inhibition and PP2A reactivation, whereas the maximal effect of DCA and SMAP combination on E98 cell viability was only 50%. However, indicative of GB cell selectivity of the drug interactions, the human fibroblasts did not show any signs of synergy between kinase inhibition and SMAPs (Fig. 4B). Additionally, the results were confirmed by colony growth assay (Fig. 4C).
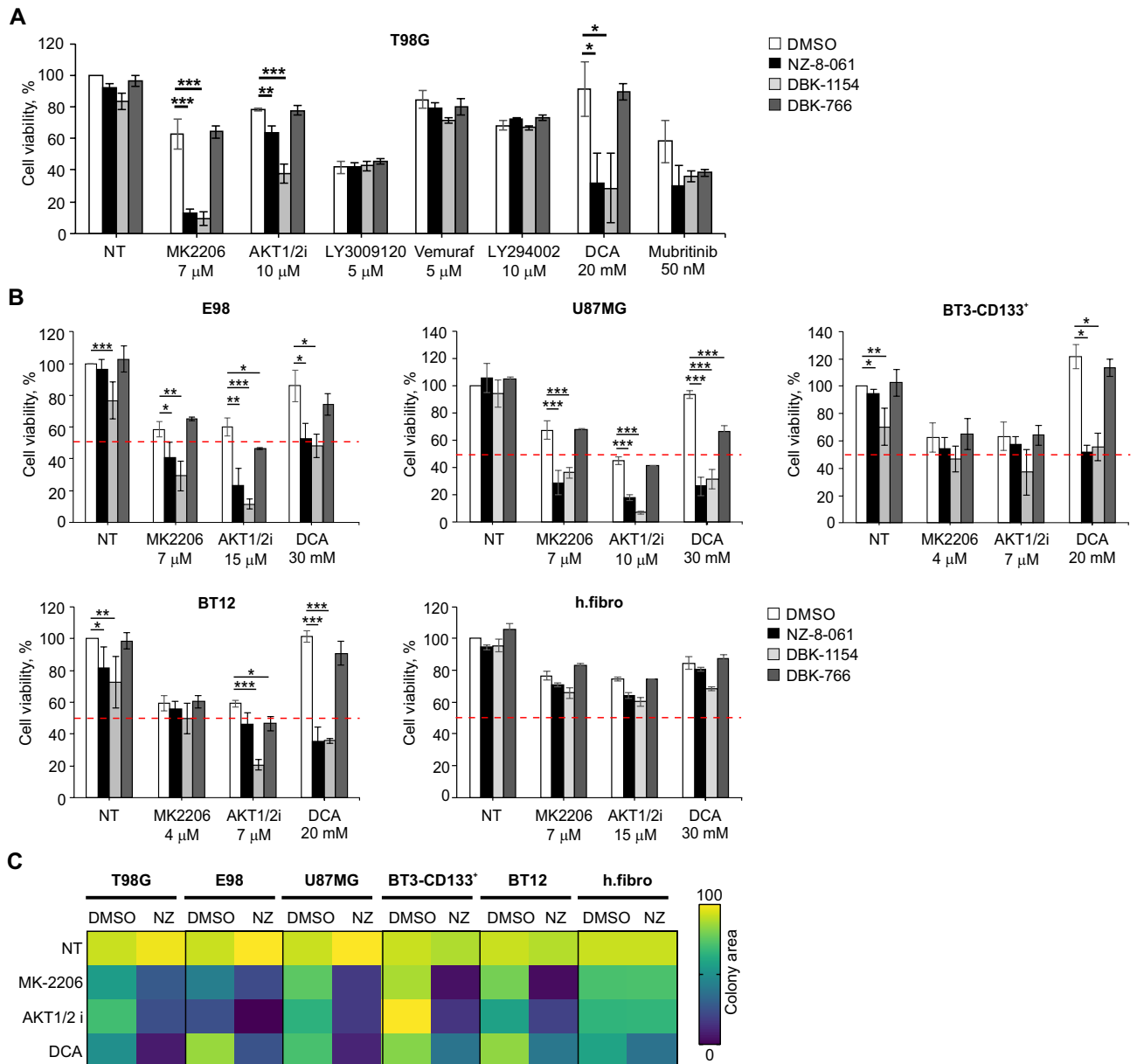
Figure 4. Exploration of AToMI results in heterogeneous GB cell lines. (**A**, **B**) Viability of T98G (**A**) and established GB, E98 and U87MG, and patient-derived GSCs, BT3-CD133^{+} and BT12, cell lines (**B**) treated with the selected kinase inhibitors alone or in combination with 8 μM NZ-8-061, 6 μM DBK-1154 or 10 μM DBK-766 for 72 h. Human fibroblasts were used as a control of normal cells. Data as mean ± SD (n = 3 independent experiments). *$p < 0.05$, **$p < 0.01$, ***$p < 0.001$ by Student's t-test. Red striped line indicates 50% inhibition of cell viability which is considered as a cytostatic but not cytotoxic response. (**C**) Heat map representation of quantified colony growth assay data in the indicated established GB cell lines, patient-derived GSCs under vehicle (DMSO) or 8 μM NZ-8-061 (NZ) treatment either alone or in combination with indicated kinase inhibitors. Human fibroblasts used as a control of normal cells. (n = 2 independent experiments).

Discussion

MKIs provide an attractive approach for simultaneously inhibiting several oncogenic kinases, and some MKIs (e.g., Sunitinib, PKC412), are clinically used as cancer therapies[2]. However, similar to more selective kinase inhibitors, all tested MKIs have thus far failed in GB clinical trials[31]. STS derivatives targeting more than 50 kinases[5] could provide a sufficiently wide polypharmacological kinase inhibitor spectrum to target GB driver mechanisms, even in the case of heterogeneous GB cell populations. However, the use of STSs as GB therapeutics is compromised by their inability to cross the BBB. To overcome these limitations and to better understand GB relevant STS target kinases, we developed the AToMI screening platform. Using the Chaperone interaction assay, we found several kinases that selectively bound to STS derivatives. Then by candidate kinases siRNA screens, we identified kinases that synergized with PP2A reactivation by either PME-1 inhibition or by SMAPs. Notably, the kinases that synergized with PP2A reactivation represent the commonly hyper activated pathways

in GB. For example, the PI3K/AKT pathway is one of the most dysregulated pathways in GB[18], and it was well presented in the siRNA screen as depletion of AKT1, AKT3 and PIK3CA synergized with PP2A reactivation. Another strongly GB associated signaling mechanism was mitochondrial glycolysis, as depletion of both PDK1 and PDK4 synergized with PP2A reactivation. However, AKT and PDK1-4 targeting monotherapies have failed to demonstrate significant survival effects in clinical trials for GB which is consistent with our results that using AKT and PDK1-4 inhibitors at doses that inhibit their target kinases has very limited effects on heterogeneous GB cell lines[27,32–34]. Also, we observed clear heterogeneity between GB cell lines in their responses to individual kinase inhibitors which highlights the need for multikinase inhibition to eradicate heterogenous cell populations from human GB tumors. The AToMI approach could clearly identify STS targets that synergize with PP2A reactivation in inhibiting viability of heterogeneous GB cells. However, as additional evidence for a high degree of resistance of GB cells towards phosphorylation-targeting therapies, even the combinations of PP2A reactivation with either AKT or PDK1-4 inhibitors failed to suppress the viability of most GB cells more than 50% which is yet considered only as a cytostatic effect. Therefore, further studies are needed to explore the therapeutic impact of the AToMI identified potential combinatorial approaches in faithful brain cancer models. For this purpose, the AToMI approach was also able to identify more selective and BBB-permeable kinase inhibitors with similar biological activity than STS.

Collectively, these results validate the usefulness of the AToMI approach for future studies aiming to characterize actionable targets of MKIs in different indications. As the individual technologies used in AToMI are interchangeable with other screening technologies we postulate that AToMI will be widely useful for addressing different biological questions.

Materials and methods

Cell culture and reagents.
The established human GB cell lines U87MG (gift from Ari Hinkkanen, University of Eastern Finland, Joensuu, Finland), E98-FM-Cherry (gift from William Leenders, Radboud Institute for Molecular Life Sciences, Nijmegen, The Netherlands) and human fibroblasts (a gift from Johanna Ivaska, Turku Bioscience, Turku, Finland) were cultured in DMEM. T98G cells (VTT Technical Research Centre of Finland, Turku, Finland) were cultured in Eagle's MEM. All growth mediums were supplemented with 10% (except fibroblasts supplemented with 20%) FBS (Biowest), 2 mM L-glutamine and penicillin (50 U/mL)/streptomycin (50 μg/mL). The patient-derived GSCs BT3-CD133+ and BT12 (gift from Pirjo Laakkonen and from Kuopio University Hospital, Kuopio, Finland) were cultured as spheroids in DMEM/F12 (Gibco) and supplemented with 2 mM L-glutamine, 2% B27-supplement (Gibco), penicillin (50 U/mL)/streptomycin (50 μg/mL), 0.01 μg/mL hFGF-β (Peprotech), 0.02 μg/mL hEGF (Peprotech) and 15 mM HEPES-buffer (Gibco). All cell cultures were maintained in a humidified atmosphere containing 5% CO_2 at 37 °C.

The following chemicals were purchased from the indicated distributors: AKT1/2 inhibitor (A6730), CEP-701 (C7869), sodium salt of dichloroacetate (DCA; 347795), lipoic acid (07039), mubritinib (SML1312), PKC412 (539648) and UCN-01 (U6508) from Sigma-Aldrich; LY3009120 (S7842) and vemurafenib (S1267) from SelleckChem; K252a (BML-EI152) and rebeccamycin (ALX-380-079) from Enzo Life Sciences; K252c (2287) from Tocris Bioscience; LY294002 (440204) from Calbiochem; and MK-2206 (HY-10358) from MedChemExpress. The compounds were dissolved in DMSO (10 mM stocks) or mQ (5M DCA) and stored at − 20 °C. SMAPs (NZ-8-061, DBK-794, DBK-1154 and DBK-766) were kindly supplied by Prof. Michael Ohlmeyer (Atux Iskay LLC, Plainsboro, NJ, USA), were dissolved in DMSO (80 mM stocks) and stored at room temperature protected from light.

Generation of PME-1 knockout T98G cells.
PPME1 deficient T98G cells were generated using CRISPR/Cas9 technology. T98G cells (4×10^4 cells) were plated into 24-well plates and transduced with lentivirus particles containing the lentiCas9-Blast plasmid (Addgene #52962). After 18 h the media were exchanged with fresh media containing blasticidin. A single cell-derived clone of T98G/Cas9 was developed and further transduced with lentivirus particles containing the pKLV-PB-U6gPPME1(BbsI)-PGKpuro2ABFP plasmid (gRNA *PPME-1* exon 14: 5'-ACTTTTCGAGTCTACAAGAGTGG, ID 183157785, FuGU, Helsinki, Finland). After 18 h the media were exchanged with fresh media, and 48 h later the media were complemented with puromycin. Cas9-expression and PME-1 knockout efficiency were evaluated by immunoblot analysis.

Cell viability assay.
Optimized numbers of cells (2.5×10^3 for T98G, U87MG and human fibroblasts or 5×10^3 for E98, BT3-CD133+ and BT12) were plated onto 96-well plates and allowed to adhere. The next day, the cells were treated with vehicle (DMSO) or the indicated compounds. After 72 h, cell viability was measured using the CellTiter-Glo assay (Promega) according to the manufacturer's instructions using a BioTek Synergy H1 plate reader (BioTek).

Colony formation assay.
Optimized numbers of cells (3×10^3 for T98G, U87MG and human fibroblasts or 10×10^3 for E98, BT3-CD133+ and BT12) were seeded in 12-well plates and allowed to adhere. Patient-derived GSCs were cultured on Matrigel (Becton Dickinson) coated plates. The next day, the cells were treated with vehicle (DMSO) or the indicated compounds. After 72 h, drug-containing media were replaced with non-drug containing medium and incubated until the control wells were confluent. Cells were fixed with ice-cold methanol and stained with a 0.2% crystal violet solution in 10% ethanol. Plates were scanned and colonies were quantified by ImageJ using the Colony area plugin[35].

Chaperone interaction assay.
LUMIER (LUminescence-based Mammalian IntERactome) with BACON (bait control) assay was performed as previously described[13]. In short, 293 T cells expressing the chaperone CDC37-Renilla (prey) luciferase were transfected with a library of 3 × FLAG-tagged bait kinases in a 96-well

plate. After two days, cells were treated with 5 μM kinase inhibitors (or DMSO) for 1 h before cell lysis with 80 μL HENG buffer (20 mM Hepes-KOH pH 7.9, 150 mM NaCl, 2 mM EDTA pH 8.0, 20 mM sodium molybdate, 0.5% Triton X-100, 5% glycerol). For assay quality, we have benchmarked the assay with well-characterized kinase inhibitors[13]. Cell lysates (60 μL) expressing each bait protein were applied to anti-FLAG (Sigma, F1804) coated 384-well plates (Greiner Bio-One, 781074), which captures the bait protein. After 3 h of incubation at 4 °C, cells were washed seven times with ice cold HENG buffer using an automated plate washer (Biotek ELx405, Biotek). 20 μl luciferase assay buffer (BioLux Gaussia Luciferase Flex Assay Kit, New England Biolabs, E3308L) was added to each well and the luminescence was measured with a multimode plate reader (Envision, Perkin Elmer). After flicking off the luciferase reagent, 20 μl of ELISA buffer (1% Tween 20, 1% goat serum, 1 × PBS) with 0.1 ng/ml anti-FLAG-HRP (Sigma, A8592) was added to each well for 1 h. Plates were washed seven times with 1 × PBS/0.05% Tween using an automated plate washer, after which 20 μl ELISA detection reagent (Super-Signal ELISA Pico Chemiluminescent Substrate, Pierce 37069) was added to each well. Luminescence was read with a multimode plate reader.

siRNA screens. A custom human kinase siRNA library containing three non-overlapping siRNAs targeting each of the 37 kinases was purchased from Qiagen (Table S3). Two independent siRNA screens were done in T98G cells. AllStars negative and AllStars Death (Qiagen) were used as negative and positive controls, respectively. In the first screen, the kinase siRNA library (120 nL of 2.5 μM siRNA stocks) was dispensed in black clear bottom tissue-culture treated 384-well plates (Corning 384 #3712) using an Echo 550 acoustic dispenser. The assay plates were used right away or used later in which case they were kept sealed at − 20 °C until use. For transfection, Opti-MEM medium (Gibco) containing Lipofectamine RNAiMAX (Invitrogen, Thermo Fisher Scientific) was added (5 μL per well) using a Multidrop Combi (Thermo Fisher Scientific), and plates were mixed for 15–30 min at room temperature. After that, T98G cells (500 cells per well) were added in 20 μL of culture medium using the Multidrop Combi. The final siRNA concentration was 12 nM. After transfection, cells were incubated at 37 °C for 48 h in the presence of 5% CO$_2$. The cells were then treated with NZ-8-061 (5 μM) for 24 h and cell proliferation was measured by CellTiter-Glo (Promega) according to the manufacturer's instructions using a PHERAstar FS plate reader (BMG Labtech). In the second screen, the kinase siRNA library in combination with the control (scrambled and AllStars negative) and PME-1 siRNA (three variants, Table S5) was dispensed as described above. Then T98G cells were seeded and incubated at 37 °C for 72 h in the presence of 5% CO$_2$. Cell proliferation was measured using CellTiter-Glo. Using the collected data for each plate, the following calculations were performed to obtain percentage inhibition values for all wells *(% inhibition = 100*((averageneg−averagesample)/(averageneg−averagepos))*, where *averageneg* is the average of negative controls (scrambled and AllStars negative siRNAs), averagesample is the average of siRNA of the screened kinase, and *averagepos* is the average of a positive control (AllStars Death siRNA)). From the siRNAs targeting the same kinase, Gene Activity Ranking Profile (GARP) score for the kinase was calculated by taking the average of two siRNAs with the highest values in inhibition data (or two lowest siRNA values from viability data)[36]. Then, the synergy scores for each kinase were computed using the Highest Single Agent model[37].

Western blotting and antibodies. Cell lysates were prepared and separated by SDS-PAGE as previously described[25]. Proteins were transferred onto nitrocellulose membranes (Bio-Rad). Membranes were blocked with 5% milk in TBS-T, followed by primary antibody incubation overnight at 4 °C. Primary antibodies: PME-1 (Santa Cruz, sc-20086, 1:1000), phospho Akt S473 (Cell Signaling, 9271, 1:1000), phospho PDHE1α S300 (Millipore, ABS194, 1:1000), β-actin (Sigma-Aldrich, A1978, 1:10,000) and GAPDH (HyTest, 5G4cc, 1:10,000). Secondary antibodies were purchased from LI-COR Biotechnology or Dako (Agilent Technologies). Membranes were scanned using an Odyssey Imager (LI-COR Biotechnology) or HRP antibodies were detected using an ECL-based Curix 60 film processor (Agfa).

Bioinformatics analysis. Cytoscape network analysis software (version 3.9.0)[38] was used to visualize the STRING interactive map of the hit kinases[39]. For calculation and visualization of synergy scores, the dose–response matrix of NZ-8-061 and UCN-01 combination data were applied to the SynergyFinder (version 2.0) web application[40].

Statistical analyses. For cell culture experiments, three biological replicates were performed, and each condition was tested in triplicate, unless otherwise specified. Data are presented as mean ± SD, and statistical analyses were performed using a two-tailed Student's *t*-test assuming unequal variances. $p < 0.05$ was considered statistically significant.

Data availability
All data associated with this study are present in the paper or the Supplementary Materials.

References
1. Klaeger, S. *et al.* The target landscape of clinical kinase drugs. *Science* **358**, eaan4368 (2017).
2. Montoya, S. *et al.* Targeted therapies in cancer: To be or not to be, selective. *Biomedicines* **9**, 1591 (2021).
3. Lin, A. *et al.* Off-target toxicity is a common mechanism of action of cancer drugs undergoing clinical trials. *Sci. Transl. Med.* **11**, eaaw8412 (2019).

4. Tang, J. *et al.* Drug target commons: A community effort to build a consensus knowledge base for drug-target interactions. *Cell Chem. Biol.* **25**, 224-229 e2 (2018).
5. Gani, O. A. & Engh, R. A. Protein kinase inhibition of clinically important staurosporine analogues. *Nat. Prod. Rep.* **27**, 489–498 (2010).
6. Kauko, O. *et al.* Phosphoproteome and drug-response effects mediated by the three protein phosphatase 2A inhibitor proteins CIP2A, SET, and PME-1. *J. Biol. Chem.* **295**, 4194–4211 (2020).
7. Kauko, O. *et al.* PP2A inhibition is a druggable MEK inhibitor resistance mechanism in KRAS-mutant lung cancer cells. *Sci. Transl. Med.* **10**, 1093 (2018).
8. Vervoort, S. J. *et al.* The PP2A-Integrator-CDK9 axis fine-tunes transcription and can be targeted therapeutically in cancer. *Cell* **184**, 3143-3162 e32 (2021).
9. Westermarck, J. Targeted therapies don't work for a reason; the neglected tumor suppressor phosphatase PP2A strikes back. *FEBS J.* **285**, 4139–4145 (2018).
10. Kaur, A. *et al.* PP2A inhibitor PME-1 drives kinase inhibitor resistance in glioma cells. *Cancer Res.* **76**, 7001–7011 (2016).
11. Sangodkar, J. *et al.* Activation of tumor suppressor protein PP2A inhibits KRAS-driven tumor growth. *J. Clin. Invest.* **127**, 2081–2090 (2017).
12. Taipale, M. Quantitative profiling of chaperone/client interactions with LUMIER assay. *Methods Mol. Biol.* **1709**, 47–58 (2018).
13. Taipale, M. *et al.* Chaperones as thermodynamic sensors of drug-target interactions reveal kinase inhibitor specificities in living cells. *Nat. Biotechnol.* **31**, 630–637 (2013).
14. Brennan, C. W. *et al.* The somatic genomic landscape of glioblastoma. *Cell* **155**, 462–477 (2013).
15. Patel, A. P. *et al.* Single-cell RNA-seq highlights intratumoral heterogeneity in primary glioblastoma. *Science* **344**, 1396–1401 (2014).
16. Jha, M. K. & Suk, K. Pyruvate dehydrogenase kinase as a potential therapeutic target for malignant gliomas. *Brain Tumor Res. Treat.* **1**, 57–63 (2013).
17. Lo, H. W. Targeting Ras-RAF-ERK and its interactive pathways as a novel therapy for malignant gliomas. *Curr. Cancer Drug Targets* **10**, 840–848 (2010).
18. McDowell, K. A., Riggins, G. J. & Gallia, G. L. Targeting the AKT pathway in glioblastoma. *Curr. Pharm. Des.* **17**, 2411–2420 (2011).
19. Anastassiadis, T., Deacon, S. W., Devarajan, K., Ma, H. & Peterson, J. R. Comprehensive assay of kinase catalytic activity reveals features of kinase inhibitor selectivity. *Nat. Biotechnol.* **29**, 1039–1045 (2011).
20. Karaman, M. W. *et al.* A quantitative analysis of kinase inhibitor selectivity. *Nat. Biotechnol.* **26**, 127–132 (2008).
21. Davis, M. I. *et al.* Comprehensive analysis of kinase inhibitor selectivity. *Nat. Biotechnol.* **29**, 1046–1051 (2011).
22. Michelakis, E. D. *et al.* Metabolic modulation of glioblastoma with dichloroacetate. *Sci. Transl. Med.* **2**, 31–34 (2010).
23. Cheng, Y. *et al.* MK-2206, a novel allosteric inhibitor of Akt, synergizes with gefitinib against malignant glioma via modulating both autophagy and apoptosis. *Mol. Cancer Ther.* **11**, 154–164 (2012).
24. Gampa, G. *et al.* Brain distribution and active efflux of three panRAF inhibitors: Considerations in the treatment of melanoma brain metastases. *J. Pharmacol. Exp. Ther.* **368**, 446–461 (2019).
25. Merisaari, J. *et al.* Monotherapy efficacy of blood-brain barrier permeable small molecule reactivators of protein phosphatase 2A in glioblastoma. *Brain Commun.* **2**, fcaa002 (2020).
26. Shariati, M. & Meric-Bernstam, F. Targeting AKT for cancer therapy. *Expert Opin. Investig. Drugs* **28**, 977–988 (2019).
27. Stacpoole, P.W. Therapeutic targeting of the pyruvate dehydrogenase complex/pyruvate dehydrogenase kinase (PDC/PDK) axis in cancer. *J. Natl. Cancer Inst.* **109** (2017).
28. Gimple, R. C., Bhargava, S., Dixit, D. & Rich, J. N. Glioblastoma stem cells: Lessons from the tumor hierarchy in a lethal cancer. *Genes Dev.* **33**, 591–609 (2019).
29. Le Joncour, V. *et al.* Vulnerability of invasive glioblastoma cells to lysosomal membrane destabilization. *EMBO Mol. Med.* **11**, e9034 (2019).
30. Mooney, J. *et al.* Current approaches and challenges in the molecular therapeutic targeting of glioblastoma. *World Neurosurg.* **129**, 90–100 (2019).
31. CruzDaSilva, E., Mercier, M. C., Etienne-Selloum, N., Dontenwill, M. & Choulier, L. A systematic review of glioblastoma-targeted therapies in phases II, III, IV clinical trials. *Cancers (Basel)* **13**, 1795 (2021).
32. Kaley, T. J. *et al.* Phase II trial of an AKT inhibitor (perifosine) for recurrent glioblastoma. *J. Neurooncol.* **144**, 403–407 (2019).
33. Wen, P. Y. *et al.* Buparlisib in patients with recurrent glioblastoma harboring phosphatidylinositol 3-kinase pathway activation: An open-label, multicenter, multi-arm, phase II trial. *J. Clin. Oncol.* **37**, 741–750 (2019).
34. Dunbar, E. M. *et al.* Phase 1 trial of dichloroacetate (DCA) in adults with recurrent malignant brain tumors. *Invest. New Drugs* **32**, 452–464 (2014).
35. Guzman, C., Bagga, M., Kaur, A., Westermarck, J. & Abankwa, D. ColonyArea: An ImageJ plugin to automatically quantify colony formation in clonogenic assays. *PLoS ONE* **9**, e92444 (2014).
36. Marcotte, R. *et al.* Essential gene profiles in breast, pancreatic, and ovarian cancer cells. *Cancer Discov.* **2**, 172–189 (2012).
37. Berenbaum, M. C. What is synergy?. *Pharmacol. Rev.* **41**, 93–141 (1989).
38. Shannon, P. *et al.* Cytoscape: A software environment for integrated models of biomolecular interaction networks. *Genome Res.* **13**, 2498–2504 (2003).
39. Szklarczyk, D. *et al.* The STRING database in 2021: Customizable protein-protein networks, and functional characterization of user-uploaded gene/measurement sets. *Nucleic Acids Res.* **49**, D605–D612 (2021).
40. Ianevski, A., Giri, A. K. & Aittokallio, T. SynergyFinder 2.0: Visual analytics of multi-drug combination synergies. *Nucleic Acids Res.* **48**, W488–W493 (2020).

Acknowledgements

Author contributions

Conception and design: O.V.D., A.K. and J.W. Experimental work: O.V.D., J.M., M.T., C.S-F. and K.W. Bioinformatic analysis: L.Y. and M.J. Resources: M.O. Writing: O.V.D., J.M., T.A. and J.W. All authors reviewed the manuscript.

Funding

Competing interests

The authors declare no competing interests.

Additional information

Supplementary Information The online version contains supplementary material available at https://doi.org/10.1038/s41598-022-18118-7.

Correspondence and requests for materials should be addressed to J.W.

Reprints and permissions information is available at www.nature.com/reprints.

Publisher's note Springer Nature remains neutral with regard to jurisdictional claims in published maps and institutional affiliations.